Journal of King Saud University – Science 34 (2022) 101762

Contents lists available at ScienceDirect

Journal of King Saud University – Science

journal homepage: www.sciencedirect.com

Original article

Amine and sulfonic acid functionalized mesoporous silica as an effective adsorbent for removal of methylene blue from contaminated water

Abeer Beagan [a,1], Khalid Alotaibi [a,b,1], Manal Almakhlafi [a], Wafaa Algarabli [a], Noouf Alajmi [a], Manal Alanazi [a], Hajer Alwaalah [a], Fatamah Alharbi [a], Riyadh Alshammari [a], Abdullah Alswieleh [a,*]

[a] *Department of Chemistry, College of Science, King Saud University, Riyadh, Saudi Arabia*
[b] *King Abdullah Institute for Nanotechnology, King Saud University, Riyadh 11451, Saudi Arabia*

ARTICLE INFO

Article history:
Received 16 June 2021
Revised 4 November 2021
Accepted 7 December 2021
Available online 13 December 2021

Keywords:
Silica nanoparticles
Water remediation
Surface functionalization
Adsorption kinetics
Adsorption isotherm

ABSTRACT

Waste effluents of textiles and leather industries are seriously causing numerous health problems. Organic dyes are one of the major contaminants of industrial wastewater. Adsorption techniques can be used effectively to remove organic dyes and treat water for human consumption. In this work, we reported a rational multistep synthesis of mesoporous silica nanoparticles (MSNs) with selectively generated active inner/external surfaces. The functional groups were incorporated into the silica surface using a combination of co-condensation and post-grafting procedures. Both amine and sulfonic acid functional groups were used to produce a total coffer of MSNs inner/outer surface by amino or sulfonic moiety denoted as [N-MSNs]-N and [S-MSNs]-S, respectively. Furthermore, bifunctional groups were also synthesised by coffering the MSNs outer surface by sulfonic acid functional groups and the inner surface with amino functional groups or vice-versa denoted as [N-MSNs]-S and [S-MSNs]-N, respectively. The efficiency of the multiple grafting strategies was evaluated for the removal of cationic dye (methylene blue (MB)) from contaminated water samples using batch method mode. The physical adsorption parameters such as pH, initial concentrations of MB, exposure time and the effect of salt concentration was examined. Moreover, the adsorption kinetic models: pseudo first order, pseudo second order and interparticle diffusion were also applied for the collected data. The highest adsorption performance was accomplished by [N-MSNs]-S sorbent with 98% extraction efficiency, whereas the lowest adsorption efficiency was observed for [N-MSNs]-N sorbent. Increasing the electrolyte concentration had led to an increase in the adsorption efficiency of all nanomaterials containing sulfonic acid. An excellent extraction efficiency was obtained when the materials were applied to spiked real water samples. These adsorbents are promising for the removal of MB from wastewater on account of their high adsorption capacity and for their resistance to the presence of other unavoidable anions in the wastewater.

1. Introduction

Organic dyes are one of the most major contaminants of wastewater. The presence of such compound are dangerous to humans health and the environment, due to their serious toxicants as carcinogens (Raj et al., 2019). Organic dyes are produced from several industrial sources such as textiles, dyestuff (Shen et al., 2011), leather tanning, paints paper and food products (Ahmad et al., 2015). These dyes are stable and have a complex molecular structure (Anuar et al., 2020). There are several techniques have been used to remove these dyes such as biological processes (Katheresan et al., 2018), ion exchange (Labanda et al., 2011), oxidation and photochemical degradation. Coagulation flocculation process have proven to be effective. However, this process is unfavorable economically (Markandeya et al., 2017; Labiadh et al., 2016). Adsorption turn out to be an efficient techniques due to its low cost, availability, high efficiency, and ease of operation (Yagub et al., 2014; Zheng et al., 2017).

The mesoporous silica nanoparticles (MSNs) have unique properties as nano adsorbent for removal organic compound, such as large surface area, good thermal and chemical stabilities, tunable

---

* Corresponding author.
E-mail address: aswieleh@ksu.edu.sa (A. Alswieleh).

[1] These authors contributed equally to this work.

Peer review under responsibility of King Saud University.

Production and hosting by Elsevier

https://doi.org/10.1016/j.jksus.2021.101762
1018-3647/

pore diameters, ease of surface modification, economical regeneration and reusability (Kachbouri et al., 2018; de Paula et al., 2021; Liang et al., 2021). Recently, Arefieva et al. reported the synthesis of amorphous silicon dioxide for removal of methylene blue from aqueous solutions (Arefieva et al., 2021). Their results showed that the samples' methylene blue adsorption activity increased as the pH of the solution increased, reaching the maximum adsorption at the point above zero charge. Parida et al. reported a novel and simple one-pot process for the synthesis of functionalized MSNs using a phosphonate based non-silane precursor (N, N′-bis[4,6-bis(diethylphosphono)-1,3,5-triazin-yl]-1,2-diaminoethane), with a surface area up to 500 $m^2\ g^{-1}$ (Parida et al., 2021). The fabricated silica nanoparticles displayed high adsorption efficiency of methylene blue with 380 mg g^{-1}.

To increase the adsorption efficiency, the surface of the adsorbent have been modified with different functional groups, such as amine, carboxylic acid and sulphonic acid. (Alswieleh, 2021; Alotaibi, 2021; Boukoussa et al., 2021; Zarezadeh-Mehrizi et al., 2016) Adlnasab et al. reported the synthesis of MSNs modified with amine to uptake anionic and cationic dyes from contaminated water and the maximum adsorption capacity was found to be 400 mg g^{-1} and 371 mg g^{-1} and for alizarin yellow and phenol red, respectively (Adlnasab et al., 2017). Boukoussa et al. described the fabrication of amine-functionalized mesoporous silica materials encapsulated in calcium alginate (ALG) as adsorbent for removing methylene blue from aqueous solution (Boukoussa et al., 2021). The maximum adsorption capacity of synthesized materials was found to be ~333 mg g^{-1}. Kao and co-workers prepared MSNs modified with carboxylic acid as adsorbent for removal methylene blue (MB) from water (Deka et al., 2014). The synthesized nanoparticles exhibited an excellent adsorption capacity for MB. Recently, Alswieleh reported the synthesise of MSNs functionalised with histidine for removal MB from contaminated water (Alswieleh, 2021). The maximum removal efficiency was found to be ~70%, with maximum amount of ~65 mg g^{-1} in basic media. Beagan reported the synthesis MSNs using the Stober method and functionalized the nanoparticles with cysteine as an effective adsorbent for removal of methylene blue from contaminated water (Beagan, 2021). The maximum adsorption efficiency of methylene blue was found 140 mg g^{-1}, in basic media.

In our present work, efforts have been made to investigate the use mesoporous silica nanoparticles (MSNs) modified with two different groups (amine and sulfonic acid) along the internal and external surfaces for removing methylene blue (MB) from contaminated water. As a first step, the synthesis of nanoparticles was carried out via Stöber process to produce MSNs with average particle size of 240 nm and 6 nm pore size, and with two functional groups (amine and sulphonic groups) to examine the possibility of their use as adsorbents. Later, the adsorption capacity was investigated under different physical adsorption parameters such as pH, initial concentrations of MB, exposure time and the added salt concentration. Moreover, the adsorption kinetic models: pseudo first order, pseudo second order and interparticle diffusion were also applied for the collected data to explain the probable mechanism of adsorption.

2. Experimental

2.1. Materials

N-Cetyltrimethylammonium bromide (CTAB, 98%), tetraethylorthosilicate (TEOS, 98%), ammonium hydroxide (28 wt%), n-hexane (HPLC grade), 3-aminopropyltriethoxysilane (APTES, >98%), (3-mercaptopropyl) trimethoxysilane (MPTMS, 95%), ethanol (HPLC grade), hydrogen peroxide solution (30%), methanol (HPLC grade), acetic acid (>99.8%) were obtained from Sigma-Aldrich. Hydrochloric acid (HCl, 36%) and sodium hydroxide were obtained from Fisher Scientific. Methylene blue (MB) and ammonium nitrate (99%) were bought from WinLab. Toluene (99.5%) was bought from BDH. All chemicals were used as received. Deionized water (DI) was obtained by ion exchange using Elga Pure Nanopore system.

2.2. Preparation of mesoporous silica nanoparticles with amine in the pores [N-MSNs]

In 170 mL an aqueous solution of CTAB (1.0 g), 7.0 cm^3 of NH_4OH was added and stirred at 40 °C. To the aqueous solution, a mixture of TEOS (5.0 cm^3), APTES (0.2 cm^3) and n-hexane (20.0 cm^3) was added within 20 min. The reaction mixture was kept under stirring for 17 h at 40 °C. The product was obtained by centrifugation and washed 6 times with DI water and methanol.

2.3. Preparation of mesoporous silica nanoparticles with thiol in the pores [S-MSNs]

In 170 mL an aqueous solution of CTAB (1.0 g), 7.0 cm^3 of NH_4OH was added and stirred at 40 °C. To the aqueous solution, a mixture of TEOS (5.0 cm^3), MPTMS (0.2 cm^3) and n-hexane (20.0 cm^3) was added within 20 min. The reaction mixture was kept under stirring for 17 h at 40 °C. The product was obtained by centrifugation and washed 6 times with DI water and methanol.

2.4. Preparation of mesoporous silica nanoparticles coated with amine [N-MSNs]-N

MSNs-NH_2 were suspended in 100.0 cm^3 solution of APTES in toluene (0.01 M) and reflexed for 20 h. The solid was separated by centrifuge and washed with toluene and ethanol. To remove the surfactant, the solid was suspended in a solution of ammonium nitrate in ethanol (15 mg cm^{-3}). Then, the mixture was stirred and heated overnight at 80 °C. The final product [N-MSNs]-N was separated by centrifuge, washed 6 times with methanol.

2.5. Preparation of mesoporous silica nanoparticles coated with sulphonic groups [S-MSNs]-S

MSNs-SH were suspended in 100.0 cm^3 solution of MPTMS in toluene (0.01 M) and reflexed for 20 h. The solid was separated by centrifuge and washed with toluene and ethanol. To remove the surfactant and convert thiols to sulphonic groups, the solid was suspended in a solution of acetic acid and hydrogen peroxide (1:1). Then, the mixture was stirred and heated overnight at 120 °C. The final product [S-MSNs]-S was separated by centrifuge, washed 6 times with methanol.

2.6. Preparation of mesoporous silica nanoparticles coated with amine in inner surface and sulphonic groups in outer surface [S-MSNs]-N

MSNs-NH_2 were suspended in 100.0 cm^3 solution of MPTMS in toluene (0.01 M) and reflexed for 20 h. The solid was separated by centrifuge and washed with toluene and ethanol. To remove the surfactant and convert thiols to sulphonic groups, the solid was suspended in a solution of acetic acid and hydrogen peroxide (1:1). Then, the mixture was stirred and heated overnight at 120 °C. The final product [S-MSNs]-N was separated by centrifuge, washed 6 times with methanol.

2.7. Preparation of mesoporous silica nanoparticles coated with sulphonic groups in inner surface and amine in outer surface [N-MSNs]-S

MSNs-SH were suspended in 100.0 cm^3 solution of APTES in toluene (0.01 M) and reflexed for 20 h. The solid was separated by centrifuge and washed with toluene and ethanol. To remove the surfactant and convert thiols to sulphonic groups, the solid was suspended in a solution of acetic acid and hydrogen peroxide (1:1). Then, the mixture was stirred and heated overnight at 120 °C. The final product [N-MSNs]-S was separated by centrifuge, washed 6 times with methanol.

2.8. Adsorption studies

The adsorption of MB on the material's surfaces were studied at varies of initial concentration (25–200 mg dm^{-3}), contact time and pH values of 3, 5, 7 and 9. The nanomaterial (10 mg) was dispersed in 10 cm^3 of an aqueous solution of MB and stirred at room temperature. The mixture was centrifuged, and MB concentration was determined using UV–vis spectrophotometer.

To calculate the adsorption capacity (q_e) at equilibrium in mg g^{-1}, equation (1) was used:

$$q_e = \frac{(C_o - C_e)V}{m} \qquad (1)$$

where V represents the volume of MB solution (dm^{-3}) and m is the mass of nanomaterials (g). C_0 and C_e are initial concentration (mg dm^{-3}) and concentration at equilibrium (mg dm^{-3}) for MB, respectively.

To investigate the adsorption behavior of MB on nanomaterials, Langmuir and Freundlich models were applied. Eq. (2) represents Langmuir model isotherm.

$$\frac{C_e}{q_e} = \frac{1}{q_m K_l} + \frac{C_e}{q_m} \qquad (2)$$

Where q_m is the maximum MB adsorption capacities (mg g^{-1}) and k_l is the Langmuir constant (dm^3 mg^{-1}).

Eq. (3) represents Freundlich model isotherm.

$$\log q_e = \frac{1}{n}\log C_e + \log K_F \qquad (3)$$

where 1/n is the adsorption intensity and K_F is the Freundlich constant ((mg g^{-1})/(mg dm^{-3})$^{1/n}$).

The adsorption kinetics was evaluated by pseudo first- and second-order. Eq. (4) represents the pseudo first-order.

$$\log(q_e - q_t) = \log(q_e) - \frac{k_1}{2.303}t \qquad (4)$$

where q_t is the adsorption capacity at time t (mg g^{-1}) and k_1 is the rate coefficient (dm^3 min^{-1}).

Eq. (5) represents the pseudo second-order.

$$\frac{t}{q_t} = \frac{1}{k_2 q_e{}^2} + \frac{1}{q_e}t \qquad (5)$$

where k_2 is the rate coefficient (g mg^{-1} min^{-1}).

2.9. Measurement and characterization

FTIR spectra were measured by Thermo Scientific Nicolet IS10 in KBr pellets in the range of 4000–400 cm^{-1} with a resolution of 4 cm^{-1}. The Scanning Electron Microscopy (SEM) and Transmission Electron Microscopy (TEM) were performed under high vacuum conditions by means of JEOL JSM-6380 LA and JEOL JEM-1230 microscopes, respectively. Elemental analysis data was collected from a Perkin Elmer Series II-2400 analyzer. UV spectra of MB was acquired by Shimadzu (UV-2600).

3. Results and discussion

3.1. Material characterization

The synthesis of MSNs was performed by the condensation reaction of silica source (TEOS)/silane agent (APTES or MPTMS) in the presence of ammonium hydroxide, templet (CTAB) and expander agent (n-hexane). The resulted MSNs were the reacted with either APTES or MPTMS to obtain amino or thiol propyl groups conveniently attached to the outer surface of MSNs. The templet was extracted using ammonium nitrate via ion exchange method, to allow the dye to interact with inner function groups.

The morphology of the nanoparticles was fully characterized using SEM and TEM techniques. As presented in Fig. 1a, the nanoparticles are roughly spherical shape. The size of the spherical particles was estimated to be 220 to 350 nm. Fig. 1b showed TEM image of the synthesized MSNs. The average particle size was estimated to be approximately 240 nm, which is close to the average particle sized estimated from SEM image. Additionally, the synthesized MSNs exhibited well-ordered porous with estimated pore size of ca. 6 nm.

Fig. 2 represent the FT-IR spectra of the fabricated nanoparticles to confirm the organic molecules attached to silica surface. For all samples, peaks were observed at 1200–1100 cm^{-1} and ~810 cm^{-1}, which apportioned to stretching of Si–O bands in silica network (Alswieleh, 2020). For surface modified MSNs, peaks were appeared at ~2900 cm^{-1} and ~1430 cm^{-1}, which were appointed C–H groups in silane agent (APTES or MPTMS), indicating the successful surface derivatization (Alswieleh et al., 2021).

To confirm the organic molecules attached to the surface of MSNs, elemental analysis was used to analyze surfactant free MSNs, [N-MSNs]-N, [S-MSNs]-S, [S-MSNs]-N, and [N-MSNs]-S. The percentages of carbon, hydrogen, nitrogen, and sulfur in the fabricated samples are presented in Table 1. It is clearly that there is an increase in the percentage of the selected elements on the functionalized nanoparticles, compared to nonmodified particles.

3.2. Adsorption studies

3.2.1. Effect of pH on adsorption

The influence of pH on the adsorption of methylene blue (MB) was studied using 10 mg of [N-MSNs]-S, [S-MSNs]-N, [N-MSNs]-N and [S-MSNs]-S with an initial MB concentration of 60 μg. dm^{-3}. The adsorption process was caried out using four different pH levels (3, 5, 7 and 9). The pH of solutions was adjusted using 0.1 M ammonia and 0.1 M hydrochloric acid. The highest adsorption performance was accomplished by [N-MSNs]-S sorbent with 98% extraction efficiency as depicted in Fig. 3. Interestingly, silica nanoparticles coated with sulfonic acid functional group [S-MSNs]-S had shown poor adsorption performance, compared to sulfonic acid moiety being only on the MSN's surface. On the other hand, 48% and 5% extraction efficiency were accomplished using [S-MSNs]-N and [N-MSNs]-N at pH 3, respectively. The key factor to understand this different adsorption behaviour is through exploring the point of zero charge (pH_{pzc}) of the studied materials and pK_a value for MB (i.e. 5.8). The pH_{pzc} of amino and sulfonic acid presented in the silica surface is ca. 7.5 and ca. 1.3, respectively. (Alswieleh, 2020; Yohai et al., 2019)

In the solution with pH < 5.8, the MB molecules will be deprotonated and exhibited a slightly negative charges that raised from the π-cloud electrons of the MB aromatic rings. Therefore, when the MB molecules approach the [S-MSNs]-S surface, some MB

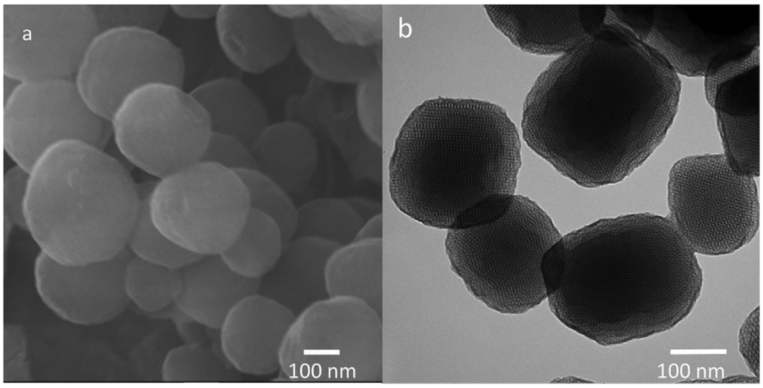

Fig. 1. Topographic images of mesoporous silica nanoparticles: (a) SEM and (b) TEM.

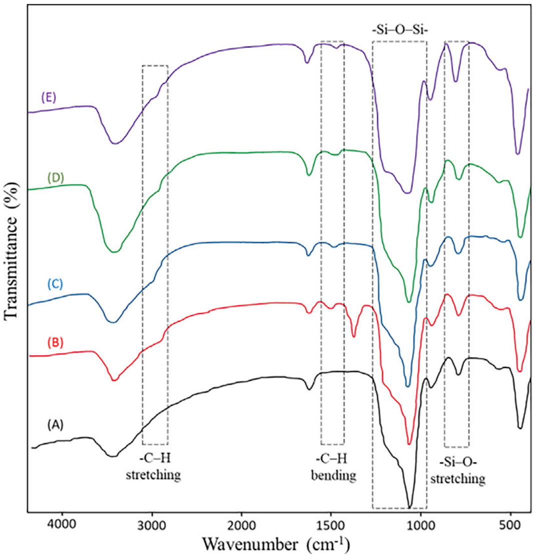

Fig. 2. FTIR spectra of: (A) surfactant free MSNs, (B) [S-MSNs]-S, (C) [N-MSNs]-N, (D) [S-MSNs]-N, and (E) [N-MSNs]-S.

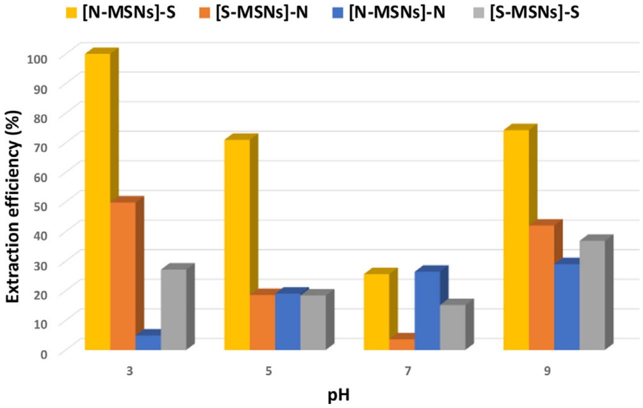

Fig. 3. Effect of solution pH on the removal of MB dye at initial MB concentration 55 ppm, sorbents mass 10 mg and volume of solution 14 cm^3.

molecules could be repelled by the material's surface, depending upon the MB molecules orientation (Bichenkova et al., 2017; Martinez and Iverson, 2012; Huber et al., 2014). In contrast, when the inner surface of the nanoparticles ([N-MSNs]-S) was modified with amino group, the negatively charged sulfonic group could be neutralized by the positively charge of protonated amino groups that present in near to the outer surface, resulting an interaction between sulfur and aromatic ring (Zauhar et al., 2000; Reid et al., 1985; Horak et al., 2004). Similar adsorption behaviour between [N-MSNs]-S and [S-MSNs]-N was observed. However, [S-MSNs]-N exhibited lower adsorption capacity which could be attributed to the present of chloride ions. The effect of increasing the chloride ions concentration on the studied materials was investigated. The results showed that the removal efficiency of amino modified MSNs ([N-MSNs]-N) was decrease as the chloride ions concentration increased. The reduction in the adsorption capacity could be attributed to the chloride ions being repelled by SO_3^- groups presented in the [N-MSNs]-S surface which was not the case with [S-MSNs]-N where the surface was covered by the protonated amino group. [N-MSNs]-N sorbent had shown poor adsorption performance, which could be attributed to the low affinity of amino group toward analyte molecules, as well as the competitive behaviour between chloride ions and MB molecules toward the available adsorption sites. The reduction in the sorbent's performance was observed as the pH level increased which can be ascribed to the gradual protonation of the MB molecule and the deprotonation of the amino group.

Table 1
Elemental analysis data of: (I) surfactant free MSNs, (II) [N-MSNs]-N, (III) [S-MSNs]-S, (IV) [S-MSNs]-N, and (V) [N-MSNs]-S.

Sample	N (%)	C (%)	H (%)	S (%)
I	–	1.27	–	–
II	1.84	7.37	1.93	–
III	0.36	8.74	2.41	1.63
IV	1.29	7.19	2.17	0.97
V	1.01	7.83	2.29	1.37

3.2.2. Effect of ionic strength on adsorption

The concentration of salt in the wastewater contained dyes is extremely high. Hence, it is of great significance to study the effects of ionic strength on the dye extraction efficiency. Therefore, in order to evaluate the effect of the salt content on the sorption of MB dye by the sorbents, NaCl was used as a model salt. Adsorption experiments were carried out by adding accurate amounts of NaCl (2.9 to 17.5 g dm^{-3}) into 14 cm^3 MB dye solution (25 µg dm^{-3}) containing 10 mg of sorbents, for 120 min, at pH = 3. As illustrated in Fig. 4, the uptake capacity of the nanoparticles contained sulfonic acid moiety have exhibited an increase in the sorption performance with increasing the salt concentration. The enhanced extraction efficiency could be attributed to the synergistic effect of the cation ions on both the analyte and the surface binding sites.

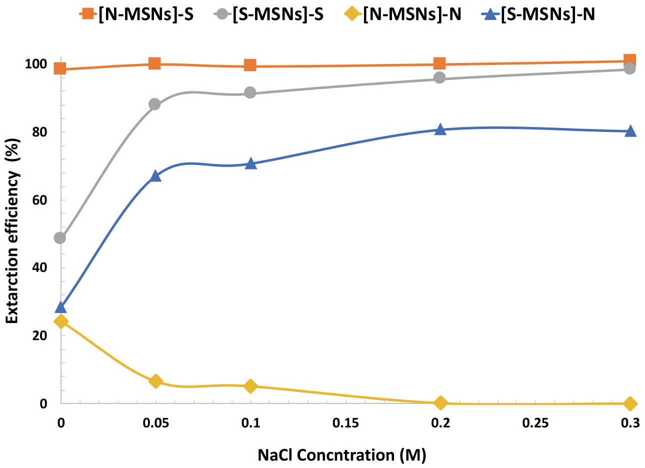

Fig. 4. Effect of solution ionic strength on the removal of MB dye at initial MB concentration 25 ppm, sorbents mass 10 mg, volume of solution 14 cm^3 and pH = 3.

Table 2
The performance of [S-MSNs]-S and [N-MSNs]-S in real water samples.

Sample	Spiked (µg cm^{-3})	Extraction efficiency (%)
[S-MSNs]-S (DI-water)	120	10.5 ± 2.3
[S-MSNs]-S (Tap-water)	120	96.2 ± 3.1
[N-MSNs]-S (DI-water)	120	48 ± 4.9
[N-MSNs]-S (Tap-water)	120	97.3 ± 2

As the addition of sodium ions leads to increasing the self-association of MB. As a result, dimer, trimer or even tetramer form of MB can reach the surface and interact with the binding sites as one supermolecule. (Fernández-Pérez and Marbán, 2020; Ghosh and Mukerjee, 1970) Furthermore, the addition of sodium ions can also eliminate the electrostatic repulsion by neutralizing the excessive negative charges on the MSNs surface, leading to more interaction between MB and binding sites at the surface. In contrast, increasing the electrolyte concentration led to decrease in the extraction efficiency of [N-MSNs]-N which could be attributed to the competition between the chloride ions and the dye molecules on the binding sites.

Henceforth, studying the adsorption capacity and the kinetic experiments are focused on the best three materials, [N-MSNs]-S, [N-MSNs]-S in NaCl (denoted as [N-MSNs]-S[Na]) and [S-MSNs]-S in NaCl (denoted as [S-MSNs]-S[Na]).

3.2.3. Evaluation of the extraction efficiency of the sorbents in real water samples

The practical performance of the selected nanomaterials was examined using real water matrices (i.e., tap water) which was collected from building 5, College of Science, King Saud University after leaving the water running for 15 min. Each experiment was repeated three times and studied under the optimal conditions. The best sorbent's performance in the present of electrolyte solution was chosen for real water sample evaluation (i.e. [N-MSNs]-S and [S-MSNs]-S). Each sample was spiked with 120 µg.cm^{-3} of MB, and the results are presented in Table 2. The extraction efficiency of the spiked samples was 96.2 and 97.3 for [S-MSNs]-S and [N-MSNs]-S, respectively. The obtained results confirm that the synthesized materials have great potential to be applied in the remediation of contaminated water solution.

Table 4
Comparison studies for MB removal from contaminated water by MSNs modified with different functional groups.

Functional group	q_e (mg g^{-1})	Ref
Amine	49	(Ge et al., 2018)
Sulfonate	208	(Zarezadeh-Mehrizi et al., 2016)
Cyclodextrin	60	(Ebadi and Rafati, 2015)
Carboxylic	43	(Jiaqi et al., 2019)
Chitosan	43	(Li et al., 2015)
Histidine	60	(Alswieleh, 2021)
[N-MSNs]-S	86.60	In this study
[N-MSNs]-S[Na]	179.04	In this study
[S-MSNs]-S[Na]	224.43	In this study

3.2.4. Equilibrium isotherms

Understanding the adsorption pathway and the equilibrium relationship between adsorbent and adsorbate is of great significance in designing adsorbents and assess their performance at the process scale. Therefore, the equilibrium adsorption isotherms are important in determining the adsorption capacity of MB and diagnose the mechanism of adsorption onto a sorbent. Langmuir and Freundlich isotherm models were utilized to describe the experimental data which corresponding to homogeneous and heterogeneous adsorbent surfaces, respectively. (Bayramoglu et al., 2012)

It can be seen in Fig. 1S, the equilibrium isotherm results confirm that Langmuir model best described the uptake of all studied materials, indicating a monolayer homogeneous adsorption of MB over the adsorbents surface. The maximum adsorption capacities of each material can be calculated according to the linearized form of Langmuir and Freundlich equations. Table 3 summarized the parameters reported form fitting data. The adsorption capacity of [S-MSNs]-S[Na] at 224.43 mg g^{-1} was significantly higher than [N-MSNs]-S and [N-MSNs]-S[Na]. The equilibrium parameter (R_L) values were all in the range of 0–1, confirms the favourable uptake of MB onto all three nanomaterials. The adsorption capacity of [S-MSNs]-S[Na] at 224.43 mg g^{-1} was significantly higher than for [N-MSNs]-S or [N-MSNs]-S[Na]. The equilibrium parameter (R_L) values were all in the range of 0–1, confirms the favourable uptake of MB onto all three adsorbents.

A comparative evaluation of [N-MSNs]-S, [N-MSNs]-S[Na] and [S-MSNs]-S[Na] and other MSNs modified functional groups for MB removal is listed in Table 4. Besides, the high adsorption capacity of suggested adsorbents toward MB compared to other materials reported in the literature, [N-MSNs]-S[Na] not only be used for cationic dye analytes but also for anionic analytes.

Table 3
Isotherm parameters for MB sorption on functionalized MSNs.

Sample	Langmuir[a]			Freundlich[a]	
	q_m (mg g^{-1})	**b** (dm^3 mg^{-1})	R_L	**K_f** (mg g^{-1})	**n** (dm^3 mg^{-1})
[N-MSNs]-S	86.60	0.37	0.10	34.39	4.62
[N-MSNs]-S[Na]	179.04	0.39	0.09	40.73	2.41
[S-MSNs]-S[Na]	224.43	0.41	0.09	48.59	1.73

[a] Reported experimental data are based upon an average value of three replicates.

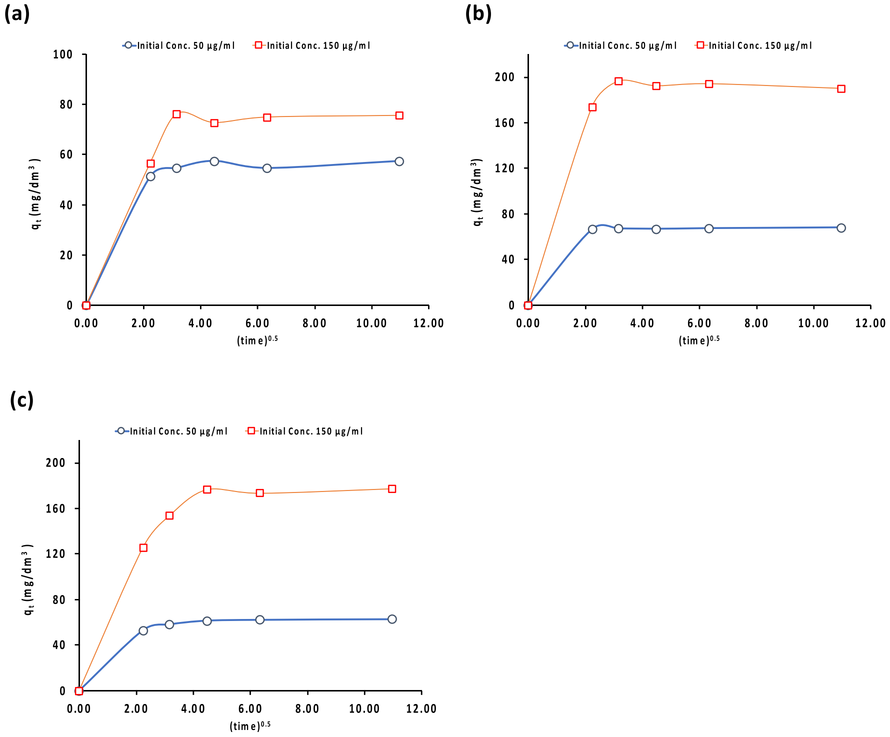

Fig. 5. Intraparticle diffusion model of (a) [N-MSNs]-S, (b) [N-MSNs]-S[Na] and (c) [S-MSNs]-S[Na].

3.2.5. Effect of adsorption time and adsorption kinetics

A kinetic study was performed to understand the MB adsorption mechanism onto the synthesised nanoparticles. Solutions with an initial MB concentration of 50 and 150 µg cm^{-3} were mixed with 10 mg of each adsorbent and the mixtures were shaken for different time intervals. Three different kinetic models were applied on the obtained data, mainly pseudo first-order, pseudo second-order and intraparticle diffusion models. By examining the pseudo-first order plots (Fig. 2S: a, c & e), the calculated correlation coefficients of 0.53, 0.23 and 0.43 indicated that the first-order model does not fit well for [N-MSNs]-S, [N-MSNs]-S [Na] and [S-MSNs]-S[Na], respectively. In contrast, the correlation coefficients of all nanomaterials were >0.99 when the data was fitted with pseudo second-order model; confirming the rate-limiting step is a chemisorption process, (Fig. 2S: b, d & f). This finding indicate that the adsorption kinetics relies upon the adsorption capacity and not on the concentration of adsorbate. (Sahoo and Prelot, 2020) Further kinetic information was observed when the intraparticle diffusion model was applied, (Fig. 5). The adsorption of MB onto all materials at low MB concentration involve one fast kinetic process, which can be explained as one-step adsorption mechanism. On the other hand, a completely different adsorption behaviour was observed at high MB concentration, as there were two-stage adsorption kinetics for [N-MSNs]-S whereas only one-step adsorption mechanism for [N-MSNs]-S-[Na], (Fig. 5a & b). This phenomenon could be explained by the fact that the MB get hindered by the negatively charged sulfonic group at the surface of [N-MSNs]-S until it reaches the neutralized area where the amino group present. In contrast, in the [N-MSNs]-S[Na] sorbent, the surface already neutralized by the cationic counterion (i.e. Na) present in the solution. Finally, three distinct kinetic steps for [S-MSNs]-S-[Na] mechanistic plot was obtained, indicating that 60% of MB was extracted as the consequence of the mass transfer effect, a second linear rate curve (5–40 min) that was believed to correspond to pore diffusion process.

The reversibility of the adsorption–desorption cycle of [N-MSNs]-S or [S-MSNs]-S was examined for MB from contaminated water. Firstly, the used adsorbents were dispersed in acidic/basic media under ultrasonication, then separated by centrifuge, washed with deionized water, and dried at 120 °C. This process has been repeated several times for each used sample. Each adsorbent was suspended in 25 ppm of MB at different pH values. Generally, it has been noticed that the removal efficiency decreased after each regeneration process, as illustrated in Fig. 3S. The removal efficiency of MB by [N-MSNs]-S decreased by ~30% at all pH values, whereas removal efficiency of MB by [S-MSNs]-S decreased by ~20% at all pH values after the second time recycling.

4. Conclusions

In this work, mesoporous silica nanoparticles (MSNs) functionalized with two different groups (amine and sulfonic acid) along the internal and external surfaces, with ~240 nm average particle size and pore size of ~6 nm have been successfully synthesized. The removal of cationic dye (methylene blue (MB)) form aqueous solution using such nanomaterials has been investigated. The highest adsorption performance was accomplished by [N-MSNs]-S sorbent with 98% extraction efficiency, whereas the lowest adsorption efficiency was observed for [N-MSNs]-N sorbents. Increasing the NaCl concentration led to an increase in the adsorption efficiency of the nanoparticles modified with all sulfonic acid moiety. The adsorption data was fitted well with Langmuir isotherm model and the best performance was accounted to [S-MSNs]-S[Na] adsorbent with 224.43 mg g^{-1} adsorption capacity. The results demonstrate that the modification of mesoporous silica nanoparticles with both sulfonic acid and amine groups could be a very promising adsorbent for the removal of both cationic and anionic dyes molecules from aqueous media.

Funding

This research received no external funding.

Declaration of Competing Interest

The authors declare that they have no known competing financial interests or personal relationships that could have appeared to influence the work reported in this paper.

Acknowledgments

The authors extend their appreciation to the Deanship of Scientific Research at King Saud University for funding this work through research group no. RG-1441-304.

Appendix A. Supplementary data

Supplementary data to this article can be found online at https://doi.org/10.1016/j.jksus.2021.101762.

References

Adlnasab, L., Shabanian, M., Ezoddin, M., Maghsodi, A., 2017. Amine rich functionalized mesoporous silica for the effective removal of alizarin yellow and phenol red dyes from waste waters based on response surface methodology. Mater. Sci. Eng., B 226, 188–198.

Ahmad, A., Mohd-Setapar, S.H., Chuong, C.S., Khatoon, A., Wani, W.A., Kumar, R., Rafatullah, M., 2015. Recent advances in new generation dye removal technologies: novel search for approaches to reprocess wastewater. RSC Adv. 5 (39), 30801–30818.

Alotaibi, K.M., 2021. Mesoporous silica nanoparticles modified with stimuli-responsive polymer brush as an efficient adsorbent for chlorophenoxy herbicides removal from contaminated water. Int. J. Environ. Anal. Chem., 1–14

Alswieleh, A.M., 2020. Modification of mesoporous silica surface by immobilization of functional groups for controlled drug release. J. Chem. 2020.

Alswieleh, A.M., 2021. Remediation of cationic and anionic dyes from water by histidine modified mesoporous silica. Int. J. Environ. Anal. Chem., 1–13

Alswieleh, A.M., Albahar, H.Y., Alfawaz, A.M., Alsilme, A.S., Beagan, A.M., Alsalme, A. M., Almeataq, M.S., Alshahrani, A., Alotaibi, K.M., 2021. Evaluation of the adsorption efficiency of glycine-, iminodiacetic acid-, and amino propyl-functionalized silica nanoparticles for the removal of potentially toxic elements from contaminated water solution. J. Nanomater. 2021.

Anuar, F., Hadibarata, T., Syafrudin, M., Fona, Z., 2020. Removal of procion red MX-5B from aqueous solution by adsorption on parkia speciosa (Stink bean) peel powder. Biointerface Res. Appl. Chem 10, 4774–4779.

Arefieva, O., Zemnukhova, L., Gorlova, V., Tsvetnov, M., 2021. Removal of methylene blue from aqueous solutions by adsorption on amorphous silicon dioxide from rice husks. Water Pract. Technol. 16 (2), 351–363.

Bayramoglu, G., Altintas, B., Arica, M.Y., 2012. Synthesis and characterization of magnetic beads containing aminated fibrous surfaces for removal of Reactive Green 19 dye: kinetics and thermodynamic parameters. J. Chem. Technol. Biotechnol. 87 (5), 705–713.

Beagan, A.M., 2021. Investigating methylene blue removal from aqueous solution by cysteine-functionalized mesoporous silica. J. Chem. 2021.

Bichenkova, E.V., Raju, A.P., Burusco, K.K., Kinloch, I.A., Novoselov, K.S., Clarke, D.J., 2017. NMR detects molecular interactions of graphene with aromatic and aliphatic hydrocarbons in water. 2D Materials 5, (1) 015003.

Boukoussa, B., Mokhtar, A., El Guerdaoui, A., Hachemaoui, M., Ouachtak, H., Abdelkrim, S., Addi, A.A., Babou, S., Boudina, B., Bengueddach, A., 2021. Adsorption behavior of cationic dye on mesoporous silica SBA-15 carried by calcium alginate beads: Experimental and molecular dynamics study. J. Mol. Liq. 333, 115976.

Deka, J.R., Lin, Y.-H., Kao, H.-M., 2014. Ordered cubic mesoporous silica KIT-5 functionalized with carboxylic acid groups for dye removal. RSC Adv. 4 (90), 49061–49069.

Ebadi, A., Rafati, A.A., 2015. Preparation of silica mesoporous nanoparticles functionalized with β-cyclodextrin and its application for methylene blue removal. J. Mol. Liq. 209, 239–245.

F.d.C. de Paula, L. Effting, G.G. Carbajal Arízaga, R.M. Giona, A.L. Tessaro, F.M. Bezerra, A. Bail, Spherical mesoporous silica designed for the removal of methylene blue from water under strong acidic conditions, Environ. Technol. (2021) 1.

Fernández-Pérez, A., Marbán, G., 2020. Visible light spectroscopic analysis of methylene blue in water; what comes after dimer? ACS Omega 5 (46), 29801–29815.

Ge, S., Geng, W., He, X., Zhao, J., Zhou, B., Duan, L., Wu, Y., Zhang, Q., 2018. Effect of framework structure, pore size and surface modification on the adsorption performance of methylene blue and Cu2+ in mesoporous silica. Colloids Surf., A 539, 154–162.

Ghosh, A.K., Mukerjee, P., 1970. Ionic strength effects on the activity coefficient of methylene blue and its self-association. J. Am. Chem. Soc. 92 (22), 6413–6415.

Horak, J., Maier, N.M., Lindner, W., 2004. Investigations on the chromatographic behavior of hybrid reversed-phase materials containing electron donor–acceptor systems: II. Contribution of π–π aromatic interactions. J. Chromatogr. A 1045 (1–2), 43–58.

Huber, R.G., Margreiter, M.A., Fuchs, J.E., von Grafenstein, S., Tautermann, C.S., Liedl, K.R., Fox, T., 2014. Heteroaromatic π-stacking energy landscapes. J. Chem. Inf. Model. 54 (5), 1371–1379.

Jiaqi, Z., Yimin, D., Danyang, L., Shengyun, W., Liling, Z., Yi, Z., 2019. Synthesis of carboxyl-functionalized magnetic nanoparticle for the removal of methylene blue. Colloids Surf., A 572, 58–66.

Kachbouri, S., Mnasri, N., Elaloui, E., Moussaoui, Y., 2018. Tuning particle morphology of mesoporous silica nanoparticles for adsorption of dyes from aqueous solution. J. Saudi Chem. Soc. 22 (4), 405–415.

Katheresan, V., Kansedo, J., Lau, S.Y., 2018. Efficiency of various recent wastewater dye removal methods: a review. J. Environ. Chem. Eng. 6 (4), 4676–4697.

Labanda, J., Sabaté, J., Llorens, J., 2011. Experimental and modeling study of the adsorption of single and binary dye solutions with an ion-exchange membrane adsorber. Chem. Eng. J. 166 (2), 536–543.

Labiadh, L., Barbucci, A., Carpanese, M.P., Gadri, A., Ammar, S., Panizza, M., 2016. Comparative depollution of Methyl Orange aqueous solutions by electrochemical incineration using TiRuSnO2, BDD and PbO2 as high oxidation power anodes. J. Electroanal. Chem. 766, 94–99.

Li, Y., Zhou, Y., Nie, W., Song, L., Chen, P., 2015. Highly efficient methylene blue dyes removal from aqueous systems by chitosan coated magnetic mesoporous silica nanoparticles. J. Porous Mater. 22 (5), 1383–1392.

Liang, S., Ziyu, Z., Han, J., Xiaoyan, D., 2021. Facile synthesis of magnetic mesoporous silica spheres for efficient removal of methylene blue via catalytic persulfate activation. Sep. Purif. Technol. 256, 117801.

Markandeya, S., Shukla, P., Mohan, D., 2017. Toxicity of disperse dyes and its removal from wastewater using various adsorbents: a review, Research Journal of. Environ. Toxicol. 11, 72–89.

Martinez, C.R., Iverson, B.L., 2012. Rethinking the term "pi-stacking". Chem. Sci. 3 (7), 2191–2201.

Parida, D., Salmeia, K.A., Sadeghpour, A., Zhao, S., Maurya, A.K., Assaf, K.I., Moreau, E., Pauer, R., Lehner, S., Jovic, M., 2021. Template-free synthesis of hybrid silica nanoparticle with functionalized mesostructure for efficient methylene blue removal. Mater. Des. 201, 109494.

Raj, S.I., Jaiswal, A., Uddin, I., 2019. Tunable porous silica nanoparticles as a universal dye adsorbent. RSC Adv. 9 (20), 11212–11219.

Reid, K., Lindley, P., Thornton, J., 1985. Sulphur-aromatic interactions in proteins. FEBS Lett. 190 (2), 209–213.

T.R. Sahoo, B. Prelot, Adsorption processes for the removal of contaminants from wastewater: the perspective role of nanomaterials and nanotechnology, Nanomaterials for the Detection and Removal of Wastewater Pollutants, Elsevier2020, pp. 161-222.

Shen, C., Shen, Y., Wen, Y., Wang, H., Liu, W., 2011. Fast and highly efficient removal of dyes under alkaline conditions using magnetic chitosan-Fe (III) hydrogel. Water Res. 45 (16), 5200–5210.

Yagub, M.T., Sen, T.K., Afroze, S., Ang, H.M., 2014. Dye and its removal from aqueous solution by adsorption: a review. Adv. Colloid Interface Sci. 209, 172–184.

Yohai, L., Mejía, H.G., Procaccini, R., Pellice, S., Kunjali, K.L., Dutta, J., Uheida, A., 2019. Nanocomposite functionalized membranes based on silica nanoparticles cross-linked to electrospun nanofibrous support for arsenic (V) adsorption from contaminated underground water. RSC Adv. 9 (15), 8280–8289.

Zarezadeh-Mehrizi, M., Badiei, A., Shahbazi, A., 2016. Sulfonate-functionalized nanoporous silica spheres as adsorbent for methylene blue. Res. Chem. Intermed. 42 (4), 3537–3551.

Zauhar, R., Colbert, C., Morgan, R., Welsh, W., 2000. Evidence for a strong sulfur–aromatic interaction derived from crystallographic data. Biopolymers 53 (3), 233–248.

Zheng, Y., Zhu, B., Chen, H., You, W., Jiang, C., Yu, J., 2017. Hierarchical flower-like nickel (II) oxide microspheres with high adsorption capacity of Congo red in water. J. Colloid Interface Sci. 504, 688–696.